Available online at www.sciencedirect.com
SCIENCE DIRECT®
Journal of Organometallic Chemistry 690 (2005) 3983–3989
Journal of Organometallic Chemistry
www.elsevier.com/locate/jorganchem

1-Triphenylstannyl-2,4,5-tritertiarybutyl-1,3-diphosphole, $Ph_3SnP_2C_3Bu^t_3$: Preparation, X-ray crystal structure, theoretical studies and solution fluxional behaviour

F. Geoffrey [a], N. Cloke [*,a], Peter B. Hitchcock [a], John F. Nixon [a,*], D. James Wilson [a], László Nyulászi [*,b], Tamás Kárpáti [b]

[a] Chemistry Department, School of Life Sciences, University of Sussex, Brighton BN1 9QJ, Sussex, UK
[b] Department of Inorganic Chemistry, Technical University of Budapest, H-1521 Budapest Gellért tér 4, Hungary

Received 17 May 2005; received in revised form 17 May 2005; accepted 26 May 2005
Available online 11 July 2005

Abstract

The 1-triphenylstannyl-2, 4, 5-tritertiarybutyl-1,3-diphosphole, $Ph_3SnP_2C_3Bu^t_3$, which has been synthesised from Ph_3SnCl and $KP_2C_3Bu^t_3$, has been fully structurally characterised in the solid state but in solution undergoes ready *intra*-molecular shifts of the Ph_3Sn-group around the 1,3-diphospholyl ring. Theoretical calculations concerning both the structure and the dynamic process are presented and discussed.

1. Introduction

Recently [1] we described the synthesis of the 5-membered aromatic 1,3-diphospholyl ring anion $P_2C_3Bu^{t-}_3$ via an unusual ring contraction reaction involving treatment of the neutral 6-membered aromatic 1,3,5-triphosphabenzene ring, $P_3C_3Bu^t_3$, with potassium (see Fig. 1).

In subsequent unpublished work [2] we have successfully utilised the resulting $K(THF)(P_2C_3Bu^t_3)$ salt in the efficient synthesis of the triad of Group 10 transition metal complexes of the type $[M(P_2C_3Bu^t_3)_2]$, (M = Ni, Pd, Pt), by treatment with the corresponding metal dichloride. However, the corresponding reactions with each of the Group 4 transition metal tetrachlorides did not lead to the expected metallocene dichlorides $[M(\eta^5\text{-}P_2C_3Bu^t_3)_2Cl_2]$, (M = Ti, Zr Hf) [3], but instead only resulted in oxidative coupling of the ring anions, yielding the known orange crystalline diphospholyl dimer, $P_4C_6Bu^t_6$ [4], as the sole product (see Fig. 2).

We therefore considered the possibility of using an organostannyl derivative of the $P_2C_3Bu^t_3$ diphospholyl ring system as an alternative synthetic approach, since the corresponding organostannyl cyclopentadiene, $R_3SnC_5H_4$, systems are well known ring transfer reagents, [5] and are readily prepared from the organotin(IV) halides, R_3SnX, and the corresponding C_5H_5 ring anion. Furthermore, Nief and Mathey [6] have utilised 1-trimethylstannyl phospholyl derivatives, such as $Me_3SnPC_5R_4$ for the preparation of a variety of η^5-complexes of the early transition metals typified by $[TiCl_3(\eta^5\text{-}PC_5R)_4]$, $[TiCl_2(\eta^5\text{-}C_5R_5)(PC_5R_4)]$ and $[TiCl_2(\eta^5\text{-}PC_5R_4)_2]$ (R = H or Me).

The NMR spectroscopically characterised 1-stannyl-1,2,4-triphospholes $R_3SnP_3C_2Bu^t_2$ (R = Me, Ph), were synthesised in our laboratory from $NaP_3C_2Bu^t_2$ and R_3SnCl, (R = Me, Ph) [7], and also by Zenneck and co-workers [8–13], in a much more comprehensive series of studies. They fully structurally characterised the latter and demonstrated its utility as a ring transfer reagent through the reactions with $SnCl_2$ generating the hexaphospha-stannocene $[Sn(\eta^5\text{-}P_3C_2Bu^t_2)_2]$ and also

* Corresponding author.
E-mail address: j.nixon@sussex.ac.uk (J.F. Nixon).

0022-328X/$ - see front matter © 2005 Elsevier B.V. All rights reserved.
doi:10.1016/j.jorganchem.2005.05.046

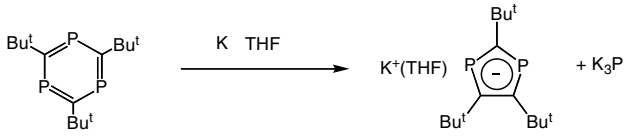

Fig. 1.

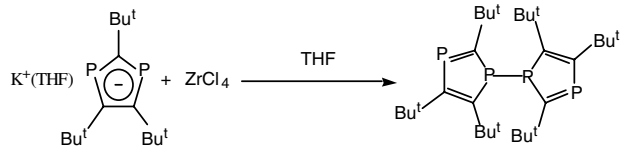

Fig. 2.

described the further synthetic potential of both the 1-triphenylstannyl and 1-trimethylstannyl 1,2,4-triphospholyl compounds in the synthesis of a variety of 1,2,4-triphospholyl transition metal derivatives of Co, Mn, Ni and Au.

2. Results and discussion

Treatment of $K(THF)(P_2C_3Bu^t_3)$ with Ph_3SnCl yielded the 1-triphenylstannyl-2,4,5-tritertiarybutyl-1,3-diphosphole $Ph_3SnP_2C_3Bu^t_3$ (**1a**) as a yellow powder. Crystals suitable for X-ray analysis were grown from a saturated slowly cooled hexane solution and the molecular structure is displayed below in Fig. 3, together with relevant bond length and bond angle data.

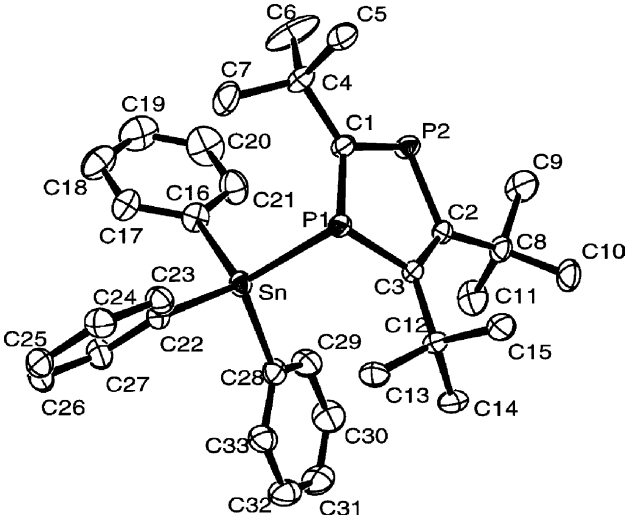

Fig. 3. Molecular structure of $Ph_3SnP_2C_3Bu^t_3$ (**1a**). Selected bond lengths (Å), and angles (°): C(1)–P(2) 1.690(3), P(2)–C(2) 1.817(3), C(2)–C(3) 1.389(4), P(1)–C(3) 1.817(3), C(1)–P(1) 1.779(3), Sn–P(1) 2.5456(9); P(1)–Sn–C(28) 113.18(9), P(1)–Sn–C(28), C(28)–Sn–C(22), C(22)–Sn–C(16), C(1)–P(1)–C(3) 99.44(14), C(1)–P(1)–Sn 97.68(10), Sn–P(1)–C(3) 97.30(10). Hydrogen atoms are omitted for clarity. Thermal ellipsoids are shown at the 50% probability level.

The structure of (**1a**) consists of a Ph_3Sn-fragment σ-bonded to an essentially planar C(1)–P(2)–C(2)–C(3)–P(1) fragment (RMS deviation of the least squares plane formed by C(1)–P(2)–C(2)–C(3)–P(1) = 0.0074). The 1-stannyldiphosphole intra-ring bond distances imply rather localised double bonds between C(3) and C(2) (1.389(4) Å) and between C(1)and P(2) (1.690(3) Å) which are, as expected, both shorter than those found in the fully delocalised π-system of the parent diphospholyl ring anion, $P_2C_3Bu^t_3{}^-$, (1.416(6) and 1.777(5) Å, respectively) [1]. The distance between C(1) and P(1) (1.779 Å), however, is somewhat shorter than a localised single bond distance which is usually greater than 1.80 Å.

The Sn atom in (**1a**) lies 2.48 Å out of the plane formed by the C(1)–P(2)–C(2)–C(3)–P(1) fragment of the diphosphole ring, and the sum of the angles around P(1) indicates strong pyramidal character, with an out of plane lone electron pair (Σ angles at P(1) = 293.42°). In the case of the 1-triphenylstannyl-1,2,4-triphosphole $Ph_3SnP_3C_2Bu^t_2$ a similar strongly pyramidalised saturated phosphorus was observed in the non-planar ring, the Sn bonded phosphorus being located 0.227(5) Å out of the best plane of the ring [11] and the sum of the angles at this saturated phosphorus centre is slightly greater (300.26°). Both values are in sharp contrast to those observed in our previously described P-substituted 1,2,4-triphospholes $(Me_3Si)_2CHP_3C_2(SiMe_3)_2$ (X), which contains a *completely planar* saturated 3-coordinate phosphorus centre [14], and in $(Me_3Si)_2CHP_3C_2Bu^t_2$ (Y) [15], where the sum of the angles at the saturated phosphorus atom is 342.0°. Compound (**1a**) represents the first example of a structurally characterised η^1-ligated $P_2C_3Bu^t_3$ ring system, although analogous compounds of the related $P_3C_2Bu^t_2$ anion are well known.

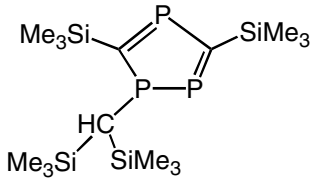

X

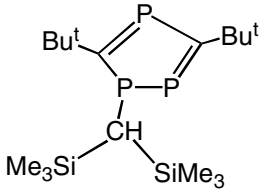

Y

We have shown elsewhere [16,17] that the aromaticity in the phosphole–pentaphosphole series becomes greater with increasing number of phosphorus atoms in the ring. Furthermore, the presence of the stannyl group on a saturated carbon was shown to substantially increase the aromaticity in cyclopentadiene [18]. In the light of these previous results the nearly unchanged (approximately 300°) bond angle sums at the saturated phosphorus atom of the stannyl substituted di- and triphospholes needs further theoretical investigation.

B3LYP/LANL2DZ(*) theoretical calculations support the non- planarity of the 1-stannyldiphosphole ring (**1a**) and calculations starting from an initial planar geometry show that the Ph_3Sn-group moves to a non-planar position. The calculated bond angle sum about phosphorus is 307°, which is somewhat larger than in the X-ray structure, however the calculated bond lengths match favourably with the X-ray data (see Table 1). With the less bulky trimethylstannyl substituent the bond angle sum is less than 300°, which is somewhat smaller than for the parent 1,3-diphosphole (301°). Since the degree of pyramidalisation at phosphorus is usually related to aromaticity in phospholes [16,17], the aromaticity measures of **1a** were compared to those of the parent 1,3-diphosphole The Bird index of **1a** was 51 (1,3-diphosphole 50) and the NICS(0) value for **1a** was −5.9 ppm (1,3-diphosphole −5.9 ppm) indicating that there is no significant change in the aromaticity of the ring upon stannyl substitution.

The effect of the stannyl group can be best understood by investigating the phosphorus non-bonding (HOMO − 1) orbital [19], which is shown for the parent 1,3-diphosphole and for its trimethylstannyl derivative in Fig. 4.

In the case of the parent 1,3-diphosphole both the π-system (at the carbon atoms) and the in-plane phosphorus lone pair contribute to the orbital. (Note that the s-type lone pair at the tri-coordinate phosphorus is situated out of the plane of the five ring atoms, and its antibonding combination with the in-plane lone pair of the phosphorus at the 3 position of the ring has the proper symmetry to overlap somewhat with the π-system.) As the number of phosphorus atoms in the ring increases, the tri-coordinate phosphorus flattens thereby allowing its p_Z orbital to overlap better with the π-system [17]. Stannyl substitution at the tri-coordinate phosphorus results in a significant perturbation of the phosphorus lone pair orbital as shown in Fig. 5. The σ_{PSn} bonding orbital which is close in energy to the phosphorus lone pair (unlike σ_{PC} which is more stable) interacts strongly, the resulting antibonding combination having similar symmetry to a p_Z type orbital. This orbital has the proper symmetry to overlap with the π-system and thus stannyl substitution at phosphorus allows an interaction between both the phosphorus lone pair and.the π-system, even with the pyramidal arrangement of phosphorus.

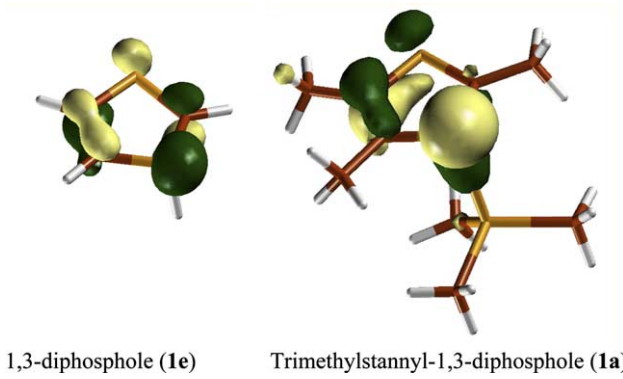

Fig. 4. HOMO − 1 phosphorus lone pair MOs of 1,3-diphosphole and its trimethylstannyl derivative.

3. Dynamic behaviour of $Ph_3SnP_2C_3Bu^t_3$ (1a)

The $^{31}P\{^1H\}$ NMR spectrum of $Ph_3SnP_2C_3Bu^t_3$ (**1a**) acquired at ambient temperature displayed two very broad resonances (δ 315, 25 ppm; $\nu_{1/2}$ = 3000 Hz) and

Table 1
B3LYP/LANL2DZ + P structural parameters and aromaticity measures of the investigated compounds QPCRPCRCR

Q	R	Isomer	*a* (Å)	*b* (Å)	*c* (Å)	*d* (Å)	*e* (Å)	ΣP (°)	Bird	NICS (ppm)	$NICS_1$ (ppm)
$SnPh_3$	*t*-Bu	**1**	1.790	1.710	1.833	1.394	1.849	307.1	46	−5.85	−5.23, −7.56
		2	1.813	1.817	1.757	1.455	1.757	–	74		
		3	1.713	1.772	1.752	1.497	1.871	–	43		
$SnMe_3$	*t*-Bu	**1**	1.790	1.711	1.833	1.395	1.844	296.9	48		
		2	1.813	1.812	1.757	1.457	1.757	–	75		
		3	1.717	1.770	1.755	1.491	1.869	–	46		
$SnMe_3$	Me	**1**	1.800	1.718	1.809	1.376	1.810	294.1	56		
		2	1.823	1.822	1.740	1.428	1.740	–	64		
		3	1.725	1.786	1.739	1.459	1.843	–	58		
$SnMe_3$	H	**1**	1.787	1.716	1.801	1.373	1.796	293.9	61		
		2	1.821	1.821	1.731	1.419	1.731	–	61		
		3	1.781	1.719	1.824	1.454	1.727	–	61		
H	H	**1**	1.795	1.703	1.820	1.363	1.804	300.7	50	−5.86	−7.05, −7.80
		2	1.866	1.866	1.708	1.442	1.708	–	30	−4.97	−7.06
		3	1.695	1.817	1.674	1.498	1.869	–	26	−3.87	−6.75

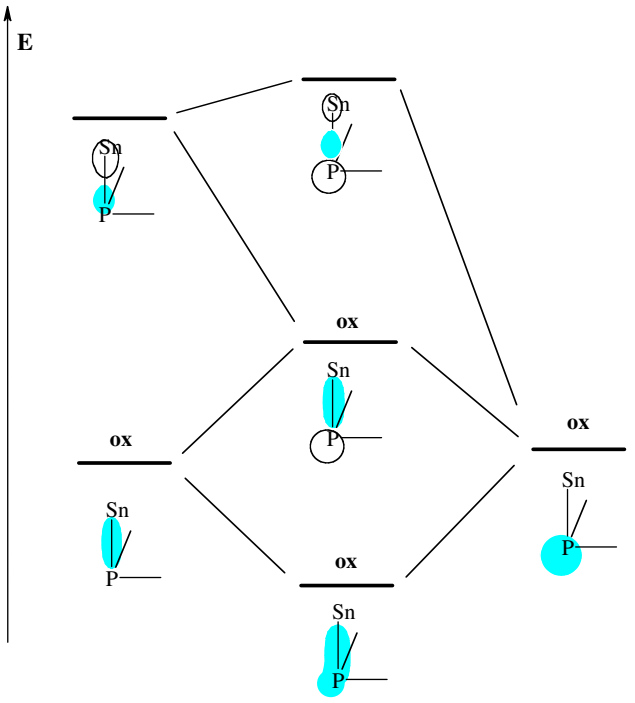

Fig. 5. Orbital interaction scheme between the P–Sn bonding (and antibonding) orbital(s) and the phosphorus lone pair.

that observed at 383 K showed a single resonance at an average of these signals (δ 160 ppm, $v_{1/2}$ = 3000 Hz) This implies a rapid exchange of the Ph_3Sn-fragment between the two phosphorus nuclei on the NMR time scale implying the existence of a dynamic process in solution. Variable temperature $^{31}P\{^1H\}$ NMR spectroscopic analysis revealed a resolution of these signals at 213 K into the expected [AX] pattern (δ 315.1 and δ 24.4 ppm $^2J(P^aP^b)$ 13.4 Hz; with tin satellites $^1J(P^aSn)$ 686.5 Hz) $^3J(P^bSn)$ 115.4 Hz; in full agreement with the solid state molecular structure.

The observation of two pseudo-triplets in the satellite sub-spectrum of the P^a resonance may be explained through virtual equivalence of the magnitudes of ^{117}Sn and ^{119}Sn phosphorus coupling. Although these two Sn spin 1/2 isotopes have different magnetogyric ratios, in practice the resulting differences in coupling to spin active hetero-nucleides is small (<5%) and averaging of the satellites is often observed. Discussions of $^1J(PSn)$ couplings usually therefore employ the averaged $^{117}Sn/^{119}Sn$ value of $^1J(SnP)$. Similarly, no resolution of the $^{117}Sn/^{119}Sn$ coupling is observed on the low field P^b resonance and the satellite sub-spectra are observed as shoulders on the main signal. The magnitude of $^1J(PSn)$ is somewhat higher than values reported for the corresponding 1-trimethylstannylphosphole derivatives such as $Me_3SnPC_4R_4$ (532–577 Hz), which are stereochemically rigid in solution and this may reflect a larger s-character in the P–Sn σ-bond of (**1a**).

The low temperature limiting spectrum of the $^{119}Sn\{^1H\}$ variable temperature NMR spectroscopic analysis, shown below in Fig. 6, displayed the pattern of lines expected for the [ABX] spin system (δ −146.2 ppm, dd, $^1J(PSn)$ 700.7 Hz; $^3J(PP)$ 124.6 Hz) in the chemical shift region for four coordinate Sn(IV) while the magnitude of $^1J(PSn)$ compares favourably with the average value deduced from the low temperature $^{31}P\{^1H\}$ NMR spectrum. Elevation of the temperature results in the collapse of the outer two signals of the [ABX] spin system resonances and the appearance of a

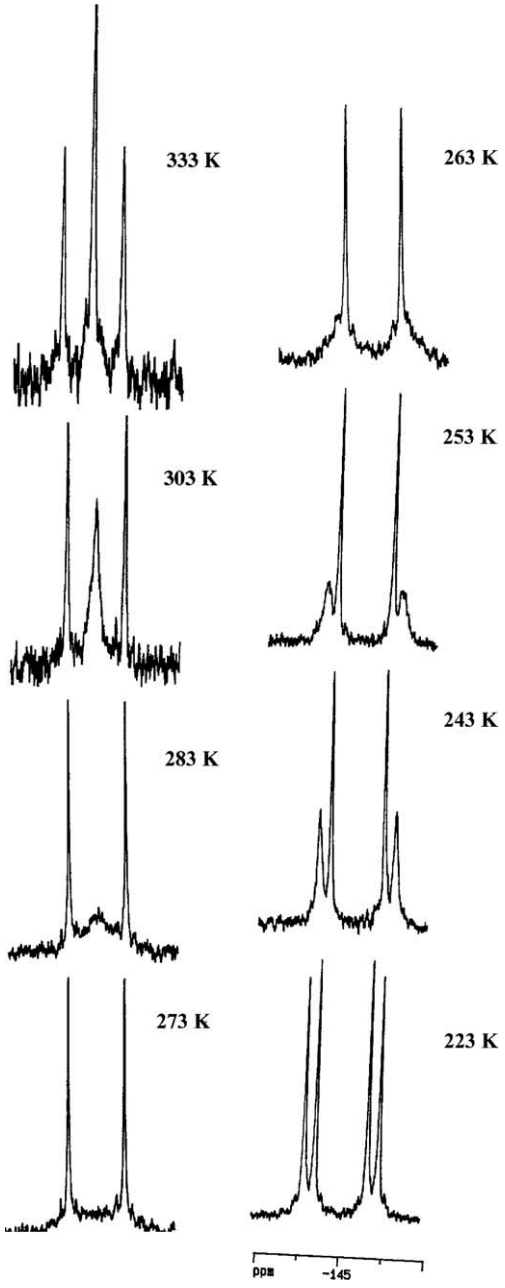

Fig. 6. Variable temperature $^{119}Sn\{^1H\}$ NMR spectra of (**1a**) (in d^8-toluene).

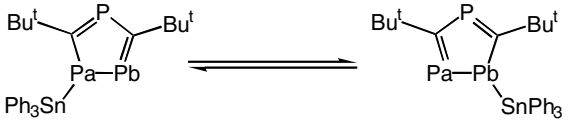

Fig. 7. sigmatropic shift in $Ph_3SnP_3C_2Bu^t_2$.

$[A_2X]$ signal bearing an averaged 1/2 ($^1J + {}^3J$) PSn scalar coupling constant. The NMR spectra thus provide strong evidence for a migration of the Ph_3Sn fragment between the two phosphorus nuclei. The coupling constants $^1J(SnP^a)$ and $^3J(SnP^b)$ were found to be opposite in sign and it is likely that $^1J(SnP^a)$ is positive by analogy with data found for 1-stannylphospholes.

Analysis of the variable temperature ^1H NMR data of (**1a**), afforded a $\Delta G^{\ddagger}$ value of 11.3 kcal/mol^{-} for this dynamic process, which is 3.9 kcal/mol^{-1} higher than the value reported by Zenneck et al. for the [1,2] migration process in $Ph_3SnP_3C_2Bu^t_2$ (see Fig. 7 below).

4. Theoretical studies concerning the mechanism of the migration process in $Ph_3SnP_2C_3Bu^t_3$ (1a)

The effect of the tin substitution on the 1,3-diphosphole ring has been investigated by theoretical methods on three sets of model compounds containing Me, ^{t}Bu, trimethylstannyl or triphenylstannyl substituents, as shown in Scheme 1. Two further isomeric structures **2** and **3** were also considered, since it can be assumed that they can be formed by an easy stannyl shift.

Recently Mathey [20] has drawn attention to the fact that the rather reactive 2H-phospholes can, in many cases, determine the reactivity of the corresponding 1H-phospholes, as a result of the easy interconversion of the two systems, by a facile H-shift. Thus, it can be expected that the reactivity of **1** will in fact be strongly influenced by the reactivity of its isomers.

Table 2
B3LYP/LANL2DZ(*) relative energies (in kcal/mol) of isomers **1**–**3** and their connecting transition structures, with different substituent patterns

	R: Me; R′: Me (c)		R: Me; R′: *t*-Bu (b)		R: Ph; R′: *t*-Bu (a)	
	ΔE	ΔG	ΔE	ΔG	ΔE	ΔG
1	0.0	0.0	0.0	0.0	0.0	0.0
2	5.8	7.6	7.5	8.0	7.5	8.8
3	10.5	12.9	13.3	14.6	13.9	16.2
TS12	9.2	11.7	7.6	8.9	9.0	10.8
TS23	11.9	14.8	14.0	14.2	19.1	20.8
TS33	16.3	19.4	20.2	21.7	26.5	28.8

First we compare the stability of **1** with respect to the possible isomeric structures **2** and **3**. The relative energies are collected in Table 2 and it is clear that the most stable isomer structure is **1** for each substituent pattern considered. Furthermore, the relative energies of the different structures show little dependence on the nature of the substituents R and R′, indicating that the steric effects must play a minor role.

All the transition structures connecting the minima are below 20 kcal/mol and the low barriers are, as expected, in accordance with the easy shift of the stannyl groups in substituted cyclopentadienes [21]. Especially noteworthy is the calculated barrier for the [1,2] H migration, being in very good agreement with the barrier concluded from the NMR investigations (see above). Thus, while **1** is the most stable structure, isomers **2** and **3** are also slightly populated and therefore, if **2** (or **3**) were to react with a substrate much faster than **1**, it would be possible to obtain products derivable from **2** (or **3**) since they can readily interconvert as shown in Fig. 8.

To understand the effects governing the relative stabilities of the isomers **1**, **2** and **3** it is necessary not only to consider the aromatic stabilisation in each, but also

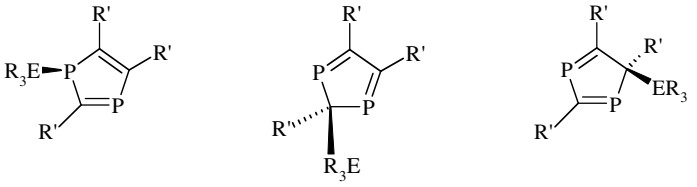

1a R: Ph R': ^{t}Bu E: Sn
1b R: Me R': ^{t}Bu E: Sn
1c R: Me R': Me E: Sn
1d R: H R': Me E: Sn
1e R: - R': H E: H

2a R: Ph R': ^{t}Bu E: Sn
2b R: Me R': ^{t}Bu E: Sn
2c R: Me R': Me E: Sn
2d R: H R': Me E: Sn
2e R: - R': H E: H

3a R: Ph R': ^{t}Bu E: Sn
3b R: Me R': ^{t}Bu E: Sn
3c R: Me R': Me E: Sn
3d R: H R': Me E: Sn
3e R: - R': H E: H

Scheme 1.

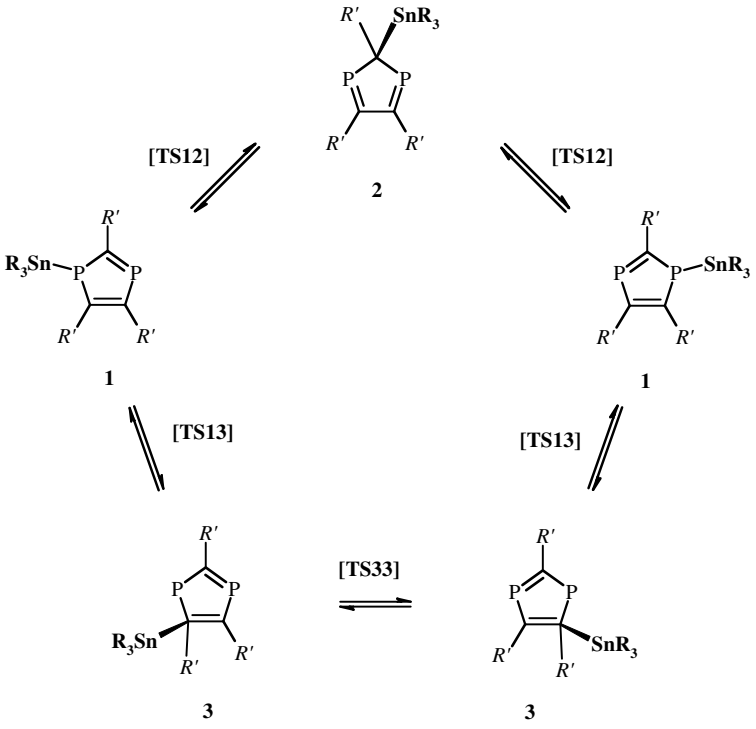

Fig. 8. Interconversion between **1**, **2** and **3** via stannyl shifts.

the importance of the strengths of the bonds between the different atoms. In isomer **1** for example there is a P–Sn bond, while in isomers **2** or **3** a C–Sn bond exists with an obviously different energy content.

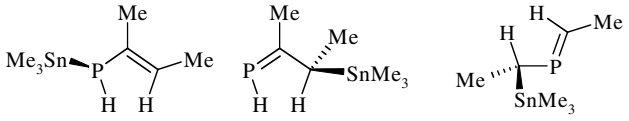

4 **5** **6**

In order to compare these two bonding situations, the structures of the isomeric compounds **4** and **5** were also calculated and the energy difference between these two structures was found to be 5.8 kcal/mol. This is of similar magnitude to the energy difference determined for **1c** and **3c** (6.2 kcal/mol). Likewise, although both **2** and **3** exhibit one SnC_{ring} bond, the position of the tetracoordinate carbon is different, since in **2** it is connected to two doubly bonded phosphorus atoms, while in **3** it is connected to only one doubly bonded phosphorus.

Compound **6** is more stable by 2.1 kcal/mol than **5**, showing the preference of the tetracoordinate carbon $C_{(Sn)}$ to be situated at an adjacent phosphorus atom. Similarly, **2** is more stable than **3** by 3.9 kcal/mol. and thus the relative energies of the isomers are mainly related to the strengths of the bonds between the different atoms and the small interactions between the neighbouring moieties, while aromaticity has a little effect on the relative energies.

5. Theoretical calculations

The density functional calculations were carried out at the B3LYP/LANL2DZ(*) level [22], by using the GAUSSIAN 98 suite of programs [23] At the optimised structures second derivatives were calculated. For the minima all second derivatives were positive (no imaginary frequencies), and for the transition structures a single negative eigenvalue of the Hessian was obtained. By following the negative eigenvector a subsequent optimisation resulted in those minima, which are connected by the transition structure.

6. Experimental section and computation

All manipulations were carried out using conventional high vacuum and Schlenk line techniques, under an atmosphere of dry argon, or under a dinitrogen atmosphere in an MBraun or Miller–Howe glove box. Solvents were refluxed over suitable drying agents, and distilled and degassed prior to use. Toluene and benzene were refluxed over sodium. Heptane and THF were refluxed over potassium. Petroleum ether (40–60 °C) and pentane were refluxed over sodium/potassium alloy. NMR solvents were dried over potassium (d_6-benzene), sodium (d_8-toluene) or calcium hydride (d_2-dichloromethane), then vacuum transferred into ampoules and stored under dinitrogen prior to use. NMR spectra were recorded on a Bruker DPX 300 or a Bruker AMX 500 spectrometer, Chemical shifts in ppm (δ) are relative

to the residual proton chemical shift of the deuterated solvent (^{1}H), the carbon chemical shift of the deuterated solvent (^{13}C) and H_3PO_4 (^{31}P) and Me_4Sn (^{119}Sn). Mass spectra were recorded on a VG autospec Fisons instrument (Electron ionisation at 70 eV) by Dr. A. Abdul-Sada. Elemental analysis was performed by Micro Analytisches Labor Pascher (Germany).

7. Synthesis of $Ph_3SnP_2C_3Bu^t_3$ (1a)

A Schlenk tube was charged with $K(THF)P_2C_3Bu^t_3$ (0.200 g, 0.526 mmol), Ph_3SnCl (0.202 g, 0.526 mmol) and THF (30 ml) and the reaction mixture was stirred for 12 h. The resulting yellow suspension was filtered through diatomaceous earth, the solvent removed in vacuo from the filtrate and the yellow oily solid recrystallised from cold hexanes yielding (**1a**) as a yellow powder (yield 0.270 g, 82%).

^{1}H NMR data (d_6-benzene, 295 K): δ 7.60–7.06 (m, 15 H, $Sn(C_6H_5)_3$), 1.47 (s, br, 18H, $CC(CH_3)_3$), 1.18 (s, 9H, $PCC(CH_3)_3P$).

$^{13}C\{^1H\}$ NMR data (d_8-toluene, 295 K): δ 202.1 (t, PCP, $J_{(PC)}$ 47.3, $^2J_{(SnC)}$ 31.16 Hz), 141.8 (p-C_6H_5, $^4J_{(SnC)}$ 4 Hz), 135.0 (*ipso*-C_6H_5, $J_{(SnC)}$ 35.6 Hz), 126.7 (o-C_6H_5, $^2J_{(SnC)}$ 6.2 Hz) 37.0 (t, $PCC(CH_3)_3P$, $^2J_{(PC)}$ 15.73 Hz), 36.4 (d, $CC(CH_3)_3C$, $^2J_{(PC)}$ 24.28 Hz), 32.7 ($PCC(CH_3)_3P$), 32.5 (br, $CC(CH_3)_3$).

$^{31}P\{^1H\}$ NMR data (d_8-toluene, 215 K): δ 315.1 (d, CP_bC, $^2J_{(PP)}$ 13.39 Hz, $^3J_{(PSn)}$ 115.4 Hz), 24.4 (d, P_aSnPh_3, $^2J_{(PP)}$ 13.39 Hz, $J_{(PSn)}$ 686.52 Hz).

$^{119}Sn\{^1H\}$ NMR data (d_8-toluene, 223 K): δ −146.2 (dd, $J_{(SnP)}$ 700.7, $^3J_{(SnP)}$ 124.6 Hz).

$^{119}Sn\{^1H\}$ NMR data (d_8-toluene, 333 K): δ −145 (t, $^2J_{(SnP)}$ 288 Hz).

EI-MS *m/z* (%): 620(55) $[M]^+$, 543 (8) $[M - Ph]^+$, 482(25) $[M(Bu^tCCBu^t)]^+$, 351(100) $[M - P_2C_3Bu^t_3]$.

7.1. Crystal data for (1a)

$C_{33}H_{42}P_2Sn$, M = 619.30, orthorhombic, space group $P2_12_12_1$, a = 8.840(2) Å, b = 17.120(5) Å, c = 20.418(6) Å, V = 3090.2(2) Å^3, T = 173(2) K, Z = 4, D_c = 1.33 Mg m^{-3}, μ = 0.95 mm^{-1}, λ = 0.71073 Å, $F(000)$ = 1280, crystal size 0.40 × 0.40 × 0.40 mm^3, 17939 measured reflections, 9001 independent reflections (R_{int} = 0.0477), 8138 reflections with $I > 2\sigma(I)$, Final indices R_1 = 0.032, wR_2 = 0.062 for $I > 2\sigma(I)$, R_1 = 0.041, wR_2 = 0.079 for all data. Data collection: Enraf Nonius CAD4. Structure solution Program package WINGX. Refinement using SHELXL-97.

Acknowledgements

The authors are grateful to the Hungarian Research Fund (OTKA Grants T 034675 and D42216) for grant support of this research. Generous allocation of computer time from the NIIF Supercomputer Centre (Budapest) is also gratefully acknowledged. J.F.N. and L.N. acknowledge joint support from the Royal Society.

References

[1] F.G.N. Cloke, P.B. Hitchcock, J.F. Nixon, D.J. Wilson, Organometallics 19 (2000) 219.
[2] F.G.N. Cloke, J.C. Green, P.B. Hitchcock, J.F. Nixon, J. Suter, D.J. Wilson, in preparation.
[3] J.R.Hanks, unpublished results, Ph.D. Thesis University of Sussex, 2000.
[4] S. Al-Juaid, P.B. Hitchcock, R.M. Matos, J.F. Nixon, J. Chem. Soc., Chem. Commun. (1993) 267.
[5] P. Jutzi, M. Kuhn, J Organomet. Chem. 173 (1979) 221;
E.C. Lund, T. Livinghouse, Organometallics 9 (1990) 2426.
[6] F. Nief, F. Mathey, J. Chem. Soc. Chem. Commun. (1998) 770.
[7] J.J. Durkin, unpublished results, Ph.D. Thesis, University of Sussex, 1995.
[8] F.W. Heinemann, H. Pritzkow, M. Zeller, U. Zenneck, Organometallics 20 (2001) 2905.
[9] M. Hofmann, F.W. Heinemann, U. Zenneck, J. Organometal. Chem. 643 (2002) 357.
[10] F.W. Heinemann, H. Pritzkow, M. Zeller, U. Zenneck, Organometallics 19 (2000) 4283.
[11] A. Elvers, F.W. Heinemann, B. Wrackmeyer, U. Zenneck, Chemistry A: Eur. J. 5 (1999) 3143.
[12] A. Elvers, F.W. Heinemann, M. Heinemann, M. Zeller, U. Zenneck, Angew. Chem. Int. Edn. Engl. 39 (2000) 2087.
[13] A. Elvers, F.W. Heinemann, S. Kummer, B. Wrackmeyer, M. Zeller, U. Zenneck, Phosphorus Sulfur Silicon and Rel. Elements 146 (1999) 725.
[14] F.G.N. Cloke, P.B. Hitchcock, P. Hunnable, J.F. Nixon, L. Nyulaszi, E. Neicke, V. Thelen, Angew. Chem. Angew. Chem., Int. Ed. Engl. 37 (1998) 1083.
[15] V. Caliman, P.B. Hitchcock, J.F. Nixon, J. Chem. Soc. Chem. Commun. (1995) 1661.
[16] L. Nyulászi, J. Phys. Chem. 100 (1996) 6194.
[17] A. Dransfeld, L. Nyulászi, P.v R. Schleyer, Inorg. Chem. 37 (1998) 4413.
[18] L. Nyulászi, P.v R. Schleyer, J. Am. Chem. Soc. 121 (1999) 6872.
[19] In Fig 4, the Kohn–Sham orbitals are shown and are essentially the same as the canonical HF MOs.
[20] F. Mathey, Acc. Chem. Res. 37 (2004) 954.
[21] Yu.A. Ustynyuk, A.V. Kisin, A.A. Zenkin, J. Organomet. Chem. 37 (1972) 101;
Yu.K. Grishin, N.M. Sergeyev, Yu.A. Ustynyuk, J. Organomet. Chem. 22 (1970) 361.
[22] d polarization fuctions with exponents 0.183, 0.55 and 0.8 were added to Sn, P and C atoms, respectively.
[23] M.J. Frisch, G.W. Trucks, H.B. Schlegel, G.E. Scuseria, M.A. Robb, J.R. Cheeseman, V.G. Zakrzewski, J.A. Montgomery Jr., R.E. Stratmann, J.C. Burant, S. Dapprich, J.M. Millam, A.D. Daniels, K.N. Kudin, M.C. Strain, O. Farkas, J. Tomasi, V. Barone, M. Cossi, R. Cammi, B. Mennucci, C. Pomelli, C. Adamo, S. Clifford, J. Ochterski, G.A. Petersson, P.Y. Ayala, Q. Cui, K. Morokuma, D.K. Malick, A.D. Rabuck, K. Raghavachari, J.B. Foresman, J. Cioslowski, J.V. Ortiz, B.B. Stefanov, G. Liu, A. Liashenko, P. Piskorz, I. Komaromi, R. Gomperts, R.L. Martin, D.J. Fox, T. Keith, M.A. Al-Laham, C.Y. Peng, A. Nanayakkara, C. Gonzalez, M. Challacombe, P.M.W. Gill, B. Johnson, W. Chen, M.W. Wong, J.L. Andres, C. Gonzalez, M. Head-Gordon, E.S. Replogle, J.A. Pople, GAUSSIAN 98, Revision A.5, Gaussian Inc., Pittsburgh, PA, 1998.